Hindawi
International Transactions on Electrical Energy Systems
Volume 2023, Article ID 9814183, 1 page
https://doi.org/10.1155/2023/9814183

Retraction

Retracted: Practical Model for Short-Circuit Current Calculation of Photovoltaic Power Station Based on Improved RLS Algorithm

International Transactions on Electrical Energy Systems

Received 12 December 2023; Accepted 12 December 2023; Published 13 December 2023

This article has been retracted by Hindawi, as publisher, following an investigation undertaken by the publisher [1]. This investigation has uncovered evidence of systematic manipulation of the publication and peer-review process. We cannot, therefore, vouch for the reliability or integrity of this article.

Please note that this notice is intended solely to alert readers that the peer-review process of this article has been compromised.

Wiley and Hindawi regret that the usual quality checks did not identify these issues before publication and have since put additional measures in place to safeguard research integrity.

We wish to credit our Research Integrity and Research Publishing teams and anonymous and named external researchers and research integrity experts for contributing to this investigation.

The corresponding author, as the representative of all authors, has been given the opportunity to register their agreement or disagreement to this retraction. We have kept a record of any response received.

References

[1] Z. Sun, M. Liu, and K. Zheng, "Practical Model for Short-Circuit Current Calculation of Photovoltaic Power Station Based on Improved RLS Algorithm," *International Transactions on Electrical Energy Systems*, vol. 2022, Article ID 5877563, 12 pages, 2022.

Hindawi
International Transactions on Electrical Energy Systems
Volume 2022, Article ID 5877563, 12 pages
https://doi.org/10.1155/2022/5877563

Research Article

Practical Model for Short-Circuit Current Calculation of Photovoltaic Power Station Based on Improved RLS Algorithm

Zhiyuan Sun, Mosi Liu, and Kun Zheng

[1]*Guangxi Key Laboratory of Intelligent Control and Maintenance of Power Equipment, Electric Power Research Institute of Guangxi Power Grid Co.Ltd., No.6-2, Minzhu Road, Xingning, Nanning 530023, Guangxi, China*

Correspondence should be addressed to Zhiyuan Sun; sun_zy.sy@gx.csg.cn and Kun Zheng; fxq8226@bistu.edu.cn

Received 1 July 2022; Revised 27 July 2022; Accepted 4 August 2022; Published 27 September 2022

Academic Editor: Raghavan Dhanasekaran

In recent years, with the rapid economic development, the development speed of all walks of life has entered a new level, and the power industry has also developed rapidly. Driven by market demand, China's power transmission range and power transmission capacity will enter a new level. At the same time, the problems brought about by the development of the power system are equally severe. Due to the large load density in individual areas, the detection of short-circuit current must be improved as an important issue. The purpose of this paper is to study how to improve the practical model of short-circuit current calculation of photovoltaic power plants, so that it can be well applied to the current high-density current detection in China. Therefore, this paper improves the recursive least squares (RLS) algorithm and applies it to the practical model of short-circuit current calculation of photovoltaic power plants and describes the improvement process of the algorithm in detail. At the same time, this paper designs relevant experiments and analysis to count the data of the improved RLS algorithm in the short-circuit current calculation of the actual photovoltaic power station and combines the data of this part to test and analyze the ability of the algorithm. The experimental results in this paper show that the improved RLS algorithm has a very good improvement in the calculation accuracy of the short-circuit current calculation of photovoltaic power plants in the actual model calculation. At the same time, the calculation efficiency is also improved, and the current tracking effect is also improved by 7%.

1. Introduction

Power short-circuit calculation makes the safety production management of power group companies in different locations more standardized and informatized. Through the establishment of the power short-circuit calculation model, the establishment of the vertical penetration and horizontal transparent safety production monitoring center of the group company is realized. During model building, one can standardize the process, behavior, and terminology standards used throughout the production business. In the operation process of electric power enterprises, the establishment of short-circuit calculation model is one of the core business contents to ensure the development of enterprises. As the connection between transmission grids becomes more and more close, the transmission network structure of UHV transmission lines will also be strengthened on the basis of the improvement of the transmission capacity of the interregional transmission network, so as to ensure the safe and reliable operation of the transmission network. In the process, unexplained short circuits are highly likely to occur during power transmission because of the limits on transmission between the various hubs. Safety requirements and the problem of excessive short-circuit currents have become one of the main problems limiting the development of transmission grids. Therefore, there is a great need to propose a segmentation operation method based on the computational power grid equivalent model.

After the reform and opening up, all walks of life in China have ushered in tremendous development, and the same is true in terms of energy. Electric energy, as one of the most important energy sources in the new century, is also

very necessary to study the fault characteristics of its current. Vikharev believed that the polymer materials used in protected wires are very sensitive to the temperature increase that occurs during short-circuit (SC) current flow. It heats the wire's insulation above the allowable temperature and may require replacement of damaged wires. Considering the periodic and aperiodic components of the SC current, he proposed a method to calculate the allowable SC current of the OHL protected wire [1]. Ma et al. obtained the three-phase short-circuit current expression of the commutated power supply by analyzing the measured short-circuit current waveform and its envelope variation law. According to the current output characteristics of the converter type power supply in different fault periods, they proposed the fault transient and steady-state equivalent circuits [2]. Xie et al. studied the fault response characteristics of the voltage-controlled inverter interface distributed generator (IIDG) and analyzed the relationship between the IIDG three-phase power and the power components in the positive and negative sequence network under asymmetric fault conditions. Then a voltage-controlled IIDG timing component model for short-circuit current calculation is established [3]. Chi et al. proposed a computational model for simulating the current fault problem and performed a parametric algorithm for it. In the course of their research, they verified the practical utility of the model through simulation experiments [4]. The mentioned researchers have made a detailed description of the short-circuit current calculation of related photovoltaic power plants, but there is no clear description of the construction of their models and the use of related algorithms.

The RLS algorithm can quickly find unknown parameters to help build models. Sun et al. proposed a recursive regularization parameter selection method for sparse RLS algorithms. The RLS algorithm they proposed is regularized by a convex function, which is equal to the linear combination of two convex functions, one dealing with random sparseness and the other dealing with group sparseness [5]. Vignesh et al. believed that an important way to improve the durability of AC power distribution systems is to use static synchronous compensators. Furthermore, except for POD, it is not only mostly discarded at the power supply level to alleviate the power quality singularity but also used for voltage control at the transmission level [6]. Kheireddine et al. solved the TEAM Workshop problem by combining the two-dimensional nonlinear finite element method and compared the results with the reference results of the classical TLBO, bat algorithm, hybrid TLBO, Nelder-Mead simplex method, and so on. The TLBO-RLS algorithm proposed by them includes a part of random local search, which can make good use of the solution space [7]. Chuku et al. proposed an electronic beam steering method for circular switched parasitic array (SPA) antennas. In a circular SPA antenna, azimuth beam steering is achieved by opening and shorting different parasitic elements; usually only one parasitic element is open at a time [8]. Through the research, we can learn from their relevant experience to improve the RLS algorithm and apply it to the calculation model of short-circuit current of photovoltaic power plants.

In the calculation of the practical model of the short-circuit current calculation of the photovoltaic power station by the previous RLS algorithm, the accuracy and efficiency of the calculation are problematic, and the short-circuit current cannot be accurately calculated. After the improvement of the RLS algorithm proposed in this paper, the calculation accuracy of its short-circuit current can be improved by 14%, which effectively improves its current calculation problem.

2. Application Method of RLS Algorithm in the Short-Circuit Current Calculation Model

2.1. Structure and Control Method of Photovoltaic Power Station. Photovoltaic power generation system is a system that converts light energy into electrical energy through the photovoltaic effect [9]. Photovoltaic power generation systems include photovoltaic panels, mechanical assembly, electrical connections, and electrical energy conversion output devices. According to whether it is interconnected with the grid, it can be divided into independent photovoltaic systems and grid-connected photovoltaic systems. Among them, grid-connected photovoltaic power station is an important form of grid-connected photovoltaic system, which converts the energy generated by photovoltaic cells through an inverter and boosts the voltage by a transformer and feeds it to the power grid.

The photovoltaic power station connected to the grid by the inverter is different from the synchronous generator type power station, and its output characteristics cannot be equivalent to the voltage source and impedance series model. Its output characteristics largely depend on the control mode of the grid-connected inverter. This chapter first introduces the basic structure of the grid-connected photovoltaic power station and the control mode of the grid-connected photovoltaic inverter [10].

2.1.1. Structure of Grid-Connected Photovoltaic Power Station. The structure of the grid-connected photovoltaic power station is shown in Figure 1, which is mainly composed of transformers, inverters, photovoltaic arrays, and supporting devices. The process of photovoltaic power generation is as follows: photovoltaic array generates direct current-confluence-inverter commutation-transformer boosting-send out [11].

Photovoltaic arrays are obtained by phasing solar panels in series and in parallel. The solar panel is obtained through the assembly of solar cells.

As the most basic unit in photovoltaic systems, solar cells directly convert solar energy into direct current. A typical solar cell structure is a PN junction made of semiconductor material, similar to a diode. The most widely used semiconductor material in solar cells is Si, which can be subdivided into two categories: amorphous silicon and crystalline silicon. Among them, the efficiency of TFPV is usually 10%–13%, and its service life is shorter than that of crystalline cells. Crystalline silicon can be divided into monocrystalline silicon and polycrystalline silicon due to different production processes. Monocrystalline silicon is

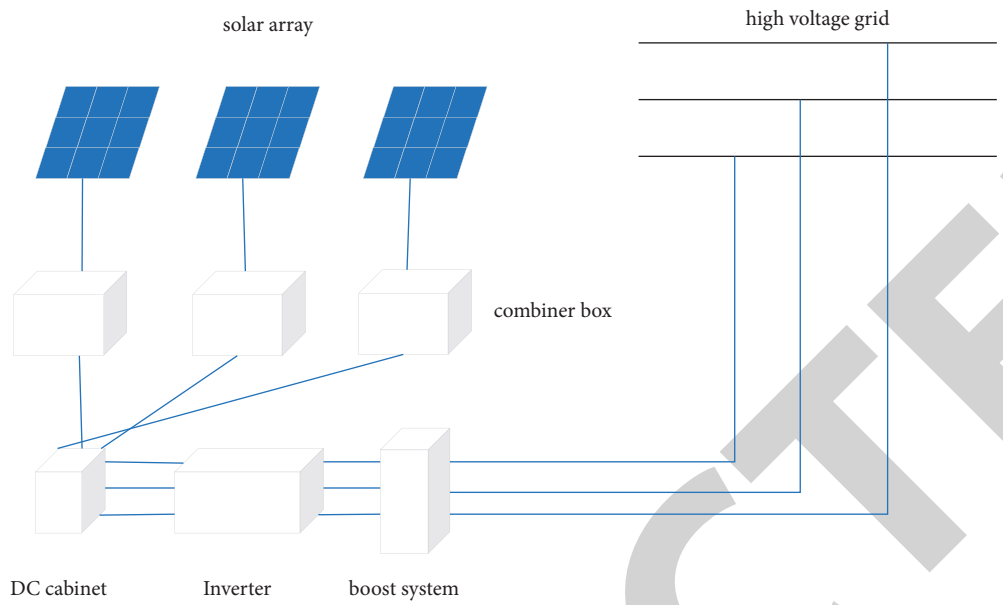

Figure 1: Composition of grid-connected photovoltaic power station.

currently the most widely used photovoltaic cell material, and the highest efficiency of monocrystalline silicon photovoltaic cells is about 23%. Cells made of polycrystalline silicon are called polycrystalline silicon cells, and the conversion efficiency of such cells is slightly lower than that of monocrystalline silicon cells. Crystalline silicon cells have high reliability and are mostly used in outdoor photovoltaic systems, with a market share of more than 70%. Figure 2 shows the appearance of several common photovoltaic modules [12].

Due to the low power of a single silicon cell, a certain number of photovoltaic cells are usually connected in series and in parallel to obtain higher output power. A certain number of photovoltaic cells are connected and sealed in the factory to form a photovoltaic module, and then one or more photovoltaic modules are connected with a common support structure to form a photovoltaic array. The voltage of the photovoltaic array is proportional to the number of series components; the current is proportional to the number of parallel components.

The performance parameters of solar cells mainly include open circuit voltage, short-circuit current, peak voltage, peak current, peak power, fill factor, conversion efficiency, and temperature coefficient of current and voltage parameters. When other parameters are determined, the output current of a photovoltaic cell depends on the voltage across it, and its typical characteristic curve is shown in Figure 3. As the voltage at the battery port increases, the output current decreases until it finally reaches zero [13].

The main parameters of solar cells are explained as follows:

(1) Peak Voltage

The peak voltage is also called the optimal working voltage. It refers to the working voltage when the solar cell sheet outputs the maximum power; the typical value of the peak voltage of a single solar cell sheet is 0.48 v.

(2) Peak Current

The peak current is also called the optimal working current of the photovoltaic cell, at which time the solar cell outputs the maximum power.

(3) Peak Power

It refers to the relationship between the maximum output power of the solar cell sheet under specific working conditions and the peak voltage and peak current. Since the peak voltage and peak current are related to the solar radiation intensity, spectral distribution, and the operating temperature of the solar cell sheet, the determination of the peak power parameters of the solar cell sheet should be carried out under the no. 101 standard conditions of the European Commission.

The MPPT algorithm was first proposed in 1968 and applied to the space photovoltaic system. After that, a variety of MPPT algorithms were proposed. Most of these algorithms automatically change the duty cycle so that the photovoltaic system can always be at the maximum power point when the operating conditions or loads suddenly change. The common algorithms of MPPT include disturbance observation method, mountain climbing method, parasitic capacitance model method, fixed voltage and current method, artificial intelligence, and other methods [14].

Hill-climbing method and disturbance observation method are two different control methods, but these two methods have the same theoretical basis. The hill-climbing method imposes a perturbation in the duty cycle α of the power converter. The observational perturbation method is to apply a perturbation to the operating voltage of the photovoltaic array. These two methods can be implemented by analog circuits or digital circuits, and it is more advantageous to use a digital signal processing unit. The disadvantage

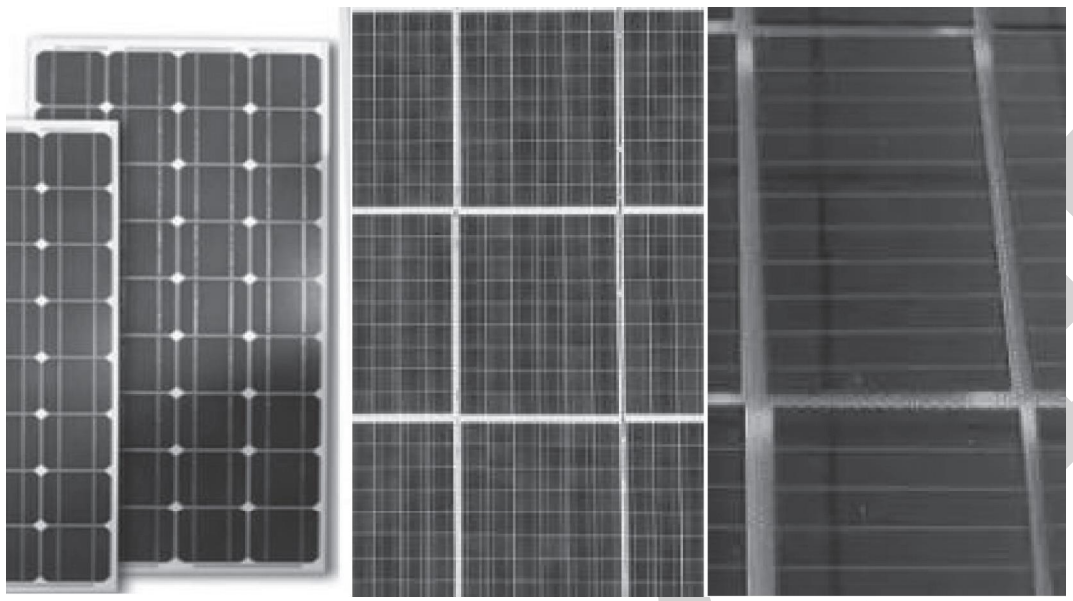

Figure 2: Appearance of PV modules.

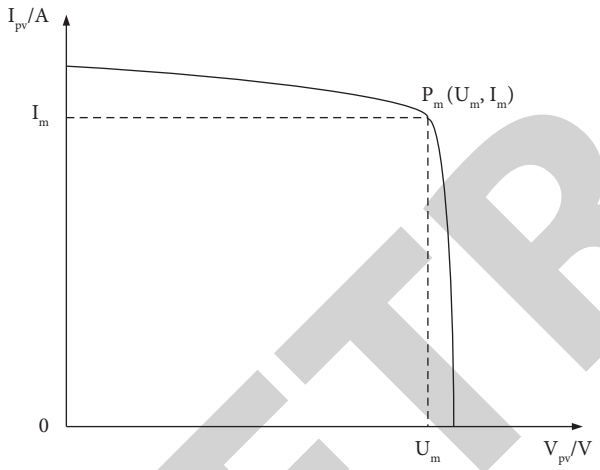

Figure 3: Typical characteristic curve.

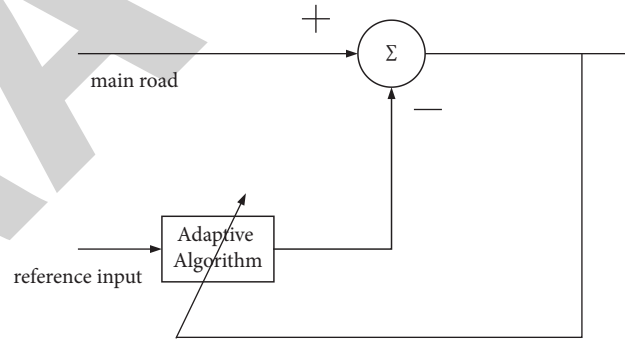

Figure 4: Principle of adaptive cancellation technology.

of the fixed voltage current method is that it needs to measure the open-circuit voltage or short-circuit current online, which will cause the output power to decrease. The advantage of the parasitic capacitance model method is that the conversion efficiency is high [15, 16]. For intelligent control technologies such as fuzzy controller, neural network, fuzzy control, and genetic algorithm, there are some other algorithms in the actual system, such as Delta adaptive method, ripple correction control (RCC), and current sweep method [17].

2.2. Current Detection Method Based on RLS Algorithm. The adaptive cancellation technology proposed in 1967 can automatically adjust the parameters of the adaptive filtering system to the best state, and the adaptive filtering algorithm is a key part of the entire ANCT [18]. Figure 4 shows the principle of ANCT.

The core of ANCT is the adaptive filtering algorithm. The most remarkable feature of the adaptive filtering algorithm is that it can effectively track the real-time changing input signal in the unknown environment according to a specific rule, so that the output signal can be optimized. Therefore, a communication system with strong real-time requirements is required. The use of adaptive filtering technology to achieve relevant real-time signal processing has a significant effect.

For stationary input signals, the cost function to be minimized is defined as $\xi(n)$, where n is the variable length of the measurable data.

$$\xi(n) = \sum_{i}^{n} e^2(i) = \min. \tag{1}$$

Let W be the tap weight vector at time n, and let $u(i)$ be the input of the tap vector at time i; they are defined as

$$W = [W_0(n), W_1(n), \ldots, W_{M-1}(n)]^T, \tag{2}$$

$$u(i) = [u(i), u(i-1), \ldots, u(i-M-1)]^T. \tag{3}$$

For nonstationary input signals, the cost function is modified as

$$\xi(n) = \sum_{i}^{n} \lambda^{n-i} e^2(i) = \sum_{i}^{n} \lambda^{n-i} \left[L(i) - W^T u(i)\right]^2 = \min. \tag{4}$$

Taking the derivative of the above formula and making it equal 0, we get

$$\frac{\partial \xi(n)}{\partial W} = -2 \sum_{i}^{n} \lambda^{n-i} e(i) u(i) = 0. \tag{5}$$

This is the orthogonal formula corresponding to the least squares criterion. After finishing the above formula, the standard formula is obtained:

$$\begin{aligned} \sum_{i=1}^{n} \lambda^{n-i} \left[L(i) - W^T u(i)\right] u(i) &= \frac{0}{W} \sum_{i=0}^{n} \lambda^{n-i} u(i) u^T(i) \\ &= \sum_{i=0}^{n} \lambda^{n-i} L(i) u(i). \end{aligned} \tag{6}$$

Define the autocorrelation matrix $R(n)$ and the cross-correlation matrix $r(n)$ as

$$R(n) = \sum_{i=0}^{n} \lambda^{n-i} u(i) u^T(i), \tag{7}$$

$$r(n) = \sum_{i=0}^{n} \lambda^{n-i} L(i) u^T(i). \tag{8}$$

Then, the standard formula can be written in simplified form:

$$R(n) W = r(n). \tag{9}$$

The solution to this formula is

$$W = R^{-1}(n) r(n). \tag{10}$$

Because W is actually a function of n, the above formula can be written as

$$W(n) = R^{-1}(n) r(n) = P(n) r(n). \tag{11}$$

$P(n)$ is defined as follows:

$$P(n) = R^{-1}(n). \tag{12}$$

To this end, it is written in the form of iterative calculation according to n, and the RLS algorithm is derived. To do this, first write formulas (7) and (8) in iterative form:

$$R(n) = \lambda R(n-1) + u(n) u^T(n), \tag{13}$$

$$r(n) = \lambda r(n-1) + L(n) u(n). \tag{14}$$

According to the above two formulas, $P(n)$ can be written as

$$P(n) = \left[\lambda P^{-1}(n-1) + u(n) u^T(n)\right]^{-1}. \tag{15}$$

Using matrix identities,

$$(A + BCD)^{-1} = A^{-1} - A^{-1} B \left(C + DA^{-1} B\right)^{-1} DA^{-1}. \tag{16}$$

$P(n)$ can be written as

$$P(n) = \frac{1}{\lambda} \left[P(n-1) - K(n) u^T(n) P(n-1)\right]. \tag{17}$$

The gain $K(n)$ in the above formula is defined as

$$K(n) = \frac{P(n-1) u(n)}{\lambda + u^T(n) P(n-1) u(n)}. \tag{18}$$

It is obtained from formula (11) that

$$W(n-1) = P(n-1) R(n-1). \tag{19}$$

Using the above formula, we can finally get

$$W(n) = W(n-1) + K(n) e(n-1). \tag{20}$$

Since $R(n)$ is a subcorrelation matrix, the appearance of the factor $P(n)$ makes the RLS algorithm have the characteristic of fast convergence.

The outstanding advantage of applying the adaptive RLS algorithm to harmonic current detection is that the initial convergence is fast. In addition, as a closed-loop detection system, it has self-adaptive ability to the changes of power grid parameters, and the algorithm has universality for single-phase and three-phase systems.

2.3. Calculation Method of the Short-Circuit Current. Harmonics or voltage and current imbalances occur during normal operation of traditional power systems. Most of them are caused by the short-circuit fault of the power grid. When the short-circuit occurs, the system transitions from the normal operation state to the fault state or the abnormal operation state. The short-circuit calculation of the power grid is a basic calculation that must be performed in order to prevent and solve a series of technologies, equipment, and material selection. The main problems are listed as follows:

(1) When designing the main wiring of a power system or power plant, it is for the selection and comparison of different schemes. Short-circuit calculations should be performed to determine whether or not to limit short-circuit currents when designing and selecting such a scheme.

(2) Select electrical equipment with sufficient thermal stability and dynamic stability, such as transformers, bus bars, porcelain bottles, and cables.

(3) Make sure there is a strong electromagnetic field around the transmission line.

(4) It is difficult to set the parameters of the relay protection device. In order to select reasonable parameters of the relay protection device and set the parameters of the automatic reclosing system correctly, this process must also go through the analysis and calculation of various faults exceeding the abnormal operating state of the power system [19–22].

The short-circuit current calculation of the microgrid has the same purpose as the traditional fault calculation, which is to solve the problem of safe and stable operation of the power grid [23]. At the same time, the calculation method of short-circuit current of photovoltaic microgrid is different from the calculation method of short-circuit current of distribution network. It is different from adding photovoltaic sources to the distribution network, so it is necessary to study the short-circuit current calculation of the microgrid and quickly and accurately calculate the fault voltage and current when calculating the asymmetric fault of the microgrid.

2.3.1. Traditional Short-Circuit Current Method

(1) Phase Component Method. With the gradual increase of the transmission distance of the distribution network, the distribution network system has certain drawbacks. The main reason is that the three-phase line parameters have a certain degree of asymmetry compared with the large power grid, and the load of the low-voltage distribution network adopts single-phase power supply, which increases the severity of the imbalance problem [24, 25]. There are other grounding methods, such as large resistance or no grounding method and grounding method through inductance coil. Under this condition, the short-circuit current calculation needs to consider the unbalance of three parameters, and the phase component method is suitable to deal with this situation [26].

When analyzing the phase components, an N-node power system network should be established, the faulty ports should be separated from the network, and Norton's equivalence should be performed. The circuit after Norton's equivalent will be greatly simplified, and the equivalent circuit shown in the figure above can be obtained after simplification. The fault side of the critical port is the Norton-equivalent circuit of the power system before the fault, and the other side of the critical port is the Norton-equivalent circuit of the phase component corresponding to the port [27]. Figure 5 shows the Norton-equivalent circuit.

2.3.2. Traditional Short-Circuit Current Calculation Structure and Model. With the extensive development of asymmetrical fault research in power grid, more and more people know the importance of short-circuit calculation, so the importance of short-circuit calculation is gradually increased. Stable operation is the main control goal of the power grid; however, the short-circuit fault of the power grid has a certain impact on the network voltage regulation and relay protection.

The short-circuit calculation results can provide the necessary basis for the normal operation of the power system and the selection of electrical equipment. It can be seen that short-circuit calculation is a particularly important basic calculation for power system analysis and an important theoretical basis for parameter setting of power system relay

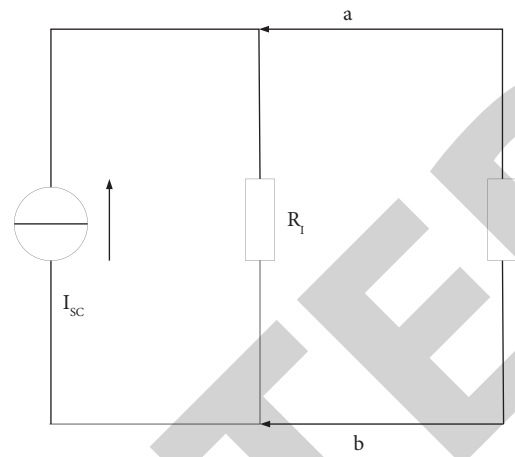

Figure 5: Norton-equivalent circuit.

protection devices. Therefore, it is of great significance to study the short-circuit calculation of the power grid for the stable operation of the power grid.

2.3.3. Influence of Fault on Photovoltaic Power Station. When the stable running system is subject to internal or external disturbance, the above-mentioned voltage and power will become unstable. Because the parameters of some energy storage elements in the system cannot be abruptly changed, the electrical quantity will not change instantaneously. At this time, the state that produces a great reverse impact on the power grid and components is called transient state:

(1) Due to the strong uncertainty of the disturbance, after the network is subjected to a small disturbance, after the transient is over, the system transitions from the original stable operation mode to another new stable operation mode. The previous safety margin is reduced.

(2) When a large disturbance occurs in the normal operation of the power system, the power system changes dramatically compared with the normal operating state, causing the current and voltage to deviate from the normal values, and the system cannot operate in the working state. As a result, the power quality obtained by the user does not meet the requirements, and even the normal power supply of the power grid will be partially or completely destroyed. If it is allowed to develop, the system will be automatically disconnected, resulting in large-scale power outages. If this state occurs, it will bring serious consequences to national defense construction, urban construction, education industry, production industry, and people's life and production. Several common power failures are shown in Figure 6.

Short-circuit analysis and calculation is an important part of power system transient analysis, and it is also one of the most basic calculations in power system analysis. In the

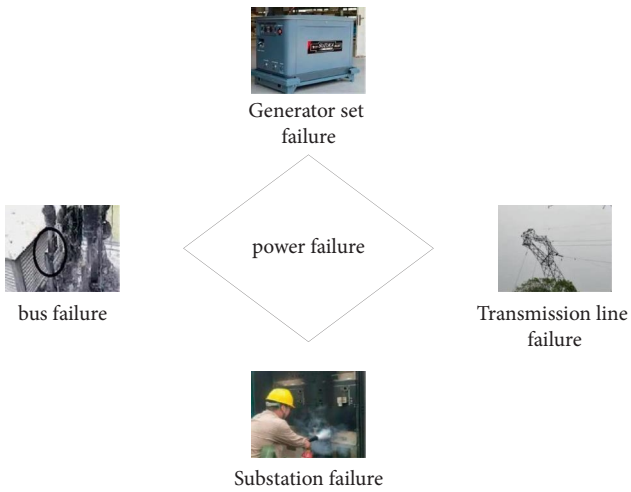

Figure 6: Several common power failures.

setting of power system parameters and the selection of equipment, short-circuit current calculation must be carried out to set parameters and select equipment according to the conclusion of the calculation. From this, we can see the importance of short-circuit current calculation. Photovoltaic power grids have many similarities with large power grids, so it is very important to calculate the faults of photovoltaic power grids. The damage of insulation in the microgrid is the main reason for short circuit, and the main reasons for this are listed as follows:

(1) Man-made accident (operating overvoltage), such as closing the switch with ground wire after the equipment fails overhaul or pulling the isolating switch with load before overhauling.

(2) Overvoltage (atmospheric overvoltage) occurring in the equipment, electrochemical aging, cracking, mechanical aging, and so forth of the insulation. Most of the causes are the failure to pay attention to some problems that are easy to cause accidents during inspection and inspection, as well as improper product design, parameter debugging, and maintenance.

The most serious fault in the short circuit is very destructive as follows:

(1) The nearby equipment is easily damaged by the high temperature attack of the short-circuit current heating or the electromagnetic force generated by the excessive fault current causes the equipment to be deformed and damaged.

(2) The voltage drops rapidly and the power shortage increases, resulting in a drop in frequency. It has caused great inconvenience to the power grid and people's lives. If the distance from the short-circuit point is far, the voltage drop will be less, but the closer the distance is, the more severe the voltage drop will be, the short-circuit point voltage is the lowest, and the direct grounding short-circuit is generally zero.

(3) Asymmetric short circuit will generate large zero-sequence voltage and zero-sequence current, and zero-sequence current will affect the sending and receiving of various signals by a large electromagnetic field. The zero-sequence voltage will produce a large voltage drop on the generator, which will seriously hinder the normal operation of the generator. Short-circuit analysis and calculation is an important part of the fault field, and it is also one of the most basic calculations in power system analysis. In the setting of power system parameters and the selection of equipment, short-circuit current calculation must be carried out to set parameters and select equipment according to the conclusion of the calculation. The photovoltaic grid is different from the distribution grid, and the microgrid has a small capacity to withstand failures. Therefore, the fault has a particularly large impact on the microgrid. In order to minimize the loss of faults or avoid the occurrence of faults, short-circuit calculations are also required to verify the stability of equipment in photovoltaic power grids.

3. Calculation Experiment of Short-Circuit Current of Distribution Networks

3.1. Calculation of Short-Circuit Current of Passive Distribution Networks. Taking the common 10 kV radiation distribution overhead line as an example, the positive and negative sequence impedances of the system power supply are equal, being j0.43. In overhead lines, the zero-sequence impedance parameter is usually 3 to 5.5 times the positive-sequence impedance. This experiment is taken as 3.5 times, and the length of the line between the two nodes is 2 km. The load impedance parameters of the nodes are shown in Table 1.

Compared with the improved RLS algorithm in this paper, the improved algorithm in this paper only needs to perform a power flow calculation to obtain the open circuit voltage, and it can converge after 6 iterations, and the iteration time is greatly shortened.

It can be seen that, for the passive distribution network, the improved port compensation algorithm considering the load effect is feasible and effective. It is relatively simple to take into account the influence of the parallel branch, and the more accurate fault current of the corresponding fault can be obtained without iterative calculation method, and the calculation is simple.

3.2. Calculation of Short-Circuit Current of Active Distribution Networks. Similarly, a synchronous generator with a rated power of 1 MW and a rated voltage of 5.7735 KV is connected to a common 10 kV distribution overhead line at the node, and the second transient reactance is j20. Also, the example model was built in DIGSILENT simulation software. It is assumed that a short-circuit occurs successively at node 1 and node 2, respectively. In this way, the program is written in MATLAB and calculated by the improved RLS algorithm in this paper. The results are shown in Table 2 and Table 3.

Table 1: Nodal load impedance parameters.

Node	Load impedance parameters (MVA)			Wiring
	Phase A (AB)	Phase B (BC)	Phase C (CA)	
1	0.451 + j0.210	0.421 + j0.196	0.395 + j0.184	△
3	0.527 + j0.246	0.421 + j0.196	0.351 + j0.164	Y
5	0.465 + j0.216	0.380 + j0.177	0.423 + j0.197	△
7	0.500 − j0.234	0.286 − j0.133	0.393 − j0.183	△

Table 2: Calculation results of short-circuit current in distributed power distribution network when one node fails.

	Ways to improve	Simulation calculation
Three-phase short-circuit current calculation results	5445.27	5447.23
Calculation error (%)	0.036	—
bc two-phase short-circuit current calculation results	4706.42	4712.11
Calculation error (%)	0.028	—
Calculation result of c-phase-ground short-circuit current	3618.28	3611.23
Calculation error (%)	0.010	—
bc two-phase grounding short-circuit current calculation result	3167.07	3174.29
Calculation error (%)	0.018	—

Table 3: Calculation results of short-circuit current in distributed power distribution network when two nodes fail.

	Ways to improve	Simulation calculation
Three-phase short-circuit current calculation results	3455.09	3416.25
Calculation error (%)	0.059	—
bc two-phase short-circuit current calculation results	2982.94	2916.23
Calculation error (%)	0.045	—
Calculation result of c-phase-ground short-circuit current	2210.93	2217.34
Calculation error (%)	0.032	—
bc two-phase grounding short-circuit current calculation result	1991.42	1993.34
Calculation error (%)	0.028	—

It can be seen from the data in the above table that when the distribution network of the photovoltaic power station contains distributed power sources, the characteristics of the transient electromotive force of the transient invariance during faults are fully utilized. It is feasible and effective to adopt the constant electromotive force model which is closer to the actual situation. In this way, for the distribution network that only contains distributed power sources, the RLS algorithm improved in this paper can still be used for calculation, which is simple and accurate.

3.3. Calculation of Short-Circuit Current of Distribution Network with Inverter-Type Distributed Power Generation. The same 10 kV distribution overhead line is used. On the basis that node 3 is connected to a synchronous generator with a rated power of 1 MW, node 1 is connected to a photovoltaic inverter power generation system with a rated power of 1 MW. The control strategy is to keep the inverter connected when the fault occurs and keep the active output power of 600 kW unchanged. When the output current reaches the maximum limit, the output power is correspondingly reduced. Similarly, the example model is built in DIGSILENT simulation software, in which the inverter adopts the same control strategy. It is supposed that a short-circuit occurs at nodes 4 and 6 successively. At this time, the program was written in MATLAB, and the RLS algorithm improved in this paper was used for calculation. The results are shown in Table 4 and Table 5.

According to the data in the table, when four basic types of faults occur at node 4 and node 6, respectively, the short-circuit current error calculated by the improved RLS algorithm in this paper is as low as 0.001%. It is basically consistent with the simulation results of DIGSILENT simulation software and is very accurate.

4. Practical Algorithms

4.1. RLS Algorithm and Improved RLS Algorithm. In order to have a better understanding of the performance of the improved RLS algorithm, this paper designs the experiment again and sets the parameters of the RLS algorithm before and after the improvement to the same parameters. For simulation experiments of two different algorithms, this paper draws the relevant data of their convergence, as shown in Figure 7.

Comparing the above two figures, we can see that the improved RLS algorithm is far superior to the previous RLS algorithm in terms of reentry convergence speed and fluctuation after convergence. It can be shown that the detection accuracy of the improved RLS algorithm is higher.

Table 4: Calculation results of short-circuit current in the case of 4-node faults in the distributed power distribution network with inverters.

	Iterative method	Simulation calculation
Three-phase short-circuit current calculation results	2413.78	2431.64
Calculation error (%)	0.000	—
bc two-phase short-circuit current calculation results	2084.66	2018.64
Calculation error (%)	0.001	—
Calculation result of c-phase-ground short-circuit current	1463.69	1429.37
Calculation error (%)	0.001	—
bc two-phase grounding short-circuit current calculation result	1376.64	1388.87
Calculation error (%)	0.002	—

Table 5: Calculation results of short-circuit current in the case of 6-node faults in the distributed power distribution network with inverters.

	Iterative method	Simulation calculation
Three-phase short-circuit current calculation results	2413.78	1824.17
Calculation error (%)	0.000	—
bc two-phase short-circuit current calculation results	2084.66	1549.67
Calculation error (%)	0.001	—
Calculation result of c-phase-ground short-circuit current	1463.69	1087.21
Calculation error (%)	0.001	—
bc two-phase grounding short-circuit current calculation result	1376.64	1039.62
Calculation error (%)	0.002	—

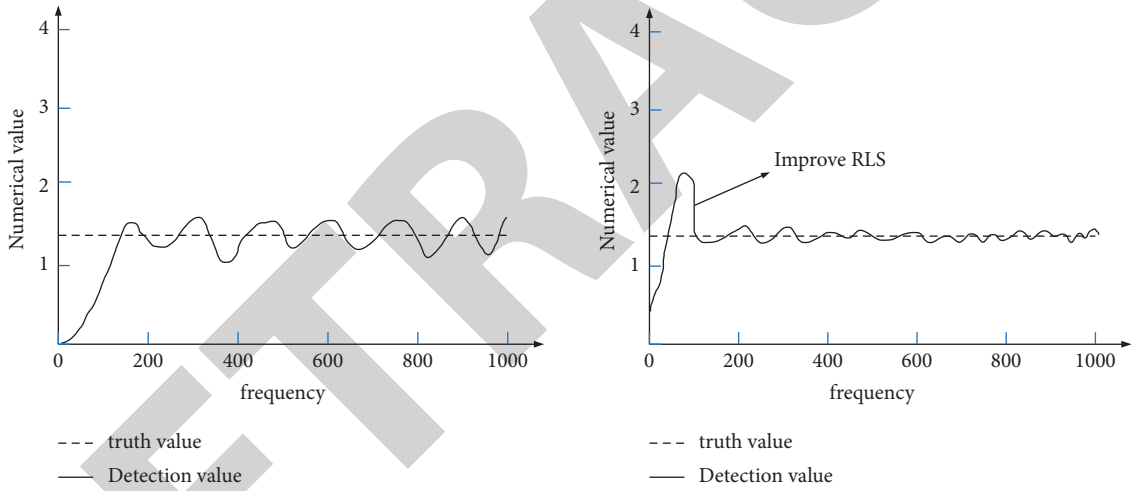

Figure 7: Waveforms of the convergence of the weights of the two algorithms.

4.2. Practical Model Simulation. In order to prove the real-time performance and feasibility of the model, the practical model is tested under three different load and power conditions by using the designed simulation model.

4.2.1. Model Simulation of Symmetrical Constant Nonlinear Load. The amplitude of the three-phase power supply voltage is equal, and the phase difference is 120°. The load is a three-phase diode rectifier bridge plus a variable resistance inductance load, and the load remains constant. Statistics of the A-phase compensation current and the grid current after compensation are shown in Figure 8.

It can be seen from the figure that when the load current does not change in a steady state, the compensated system current is always in the same phase as the power supply voltage and changes smoothly, which is very stable. Although there are six ripples in the DC bus voltage, but based on the filtering characteristics of the RLS adaptive algorithm, the final output is almost zero, which greatly reduces the influence on the calculation of the instantaneous reference value of the fundamental active current. In this way, the active power required by the load is completely provided by the power supply current, which not only achieves the filtering purpose but also controls the DC bus voltage.

4.2.2. System Simulation of Symmetrical Variable Nonlinear Load. The amplitude of the three-phase power supply voltage is equal, the phase difference is 120°, and the load is a three-phase diode rectifier bridge plus a variable resistance inductance load. The load changes at the 0.04 s current zero crossing. This varying nonlinear load simulates reactive and harmonic power, resulting in reactive and harmonic currents in the current. Statistics related data are shown in Figure 9.

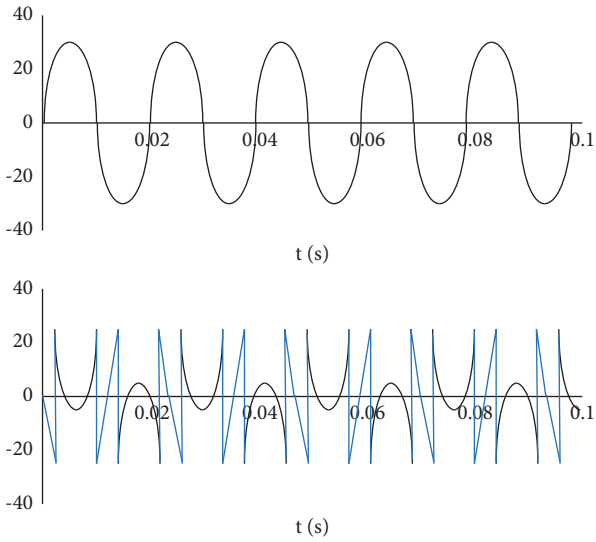

Figure 8: Comparison of A-phase compensation current and compensated current.

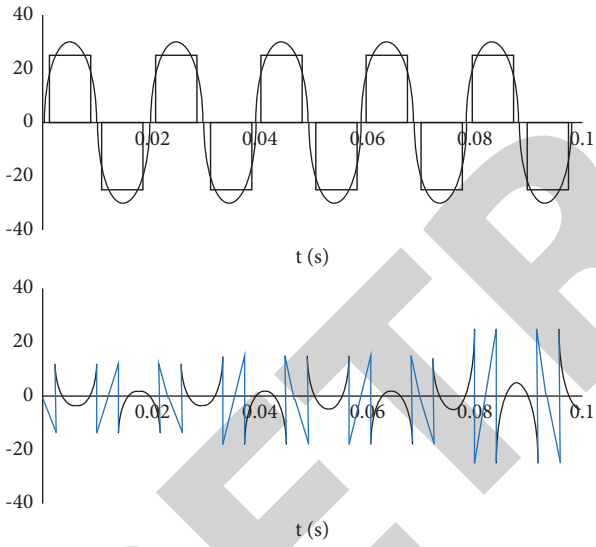

Figure 9: A-phase compensation current and compensated load current.

It can be seen that when the load current changes in amplitude, based on the rapid convergence of the RLS algorithm, the current quickly tracks the DC bus voltage change, and the SAPF can control the voltage at a very fast speed to keep it constant. In this way, when the load changes, the active energy is first provided by the capacitor, and then the capacitor is replenished from the power grid immediately, which basically achieves the purpose of real-time compensation. The compensated system current can always track the load changes quickly and smoothly and finally converges stably.

4.3. Short-Circuit Fault Characteristics. Taking a stand-alone system as an example, the short-circuit capacity of the substation is set to 240MVA, the impedance ratio of the upstream and downstream lines of the IIDG access point is

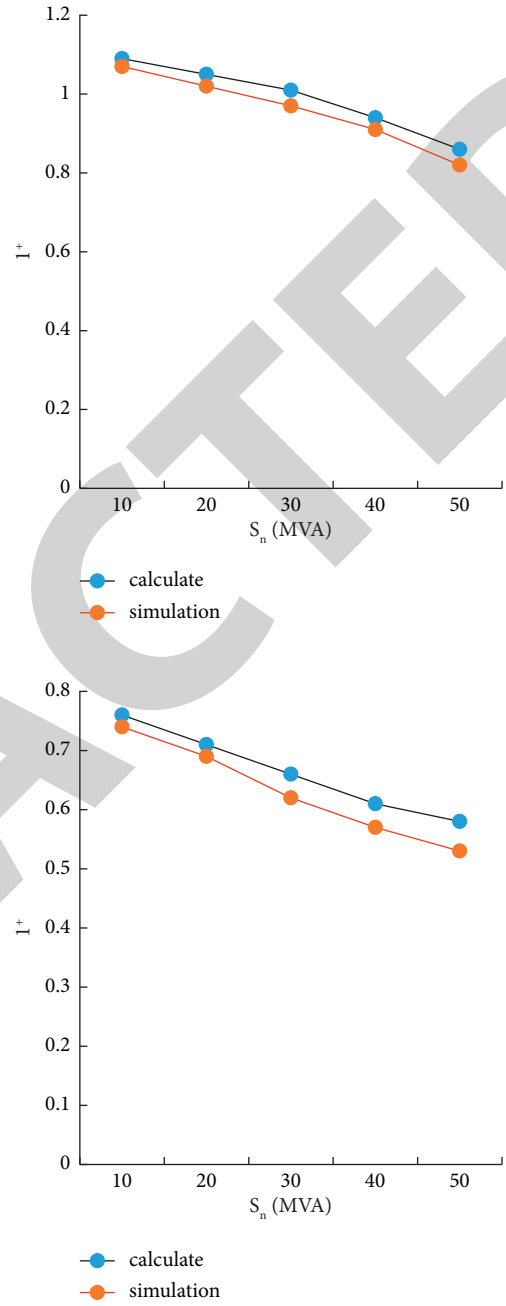

Figure 10: Converter short-circuit current for different short-circuit types and control parameters.

4, and the control parameters $P_0^* = 0.8$ pu, $Q_0^* = 0.6$ pu, $a = 1$, and kq = 1. When a two-phase short-circuit ground fault occurs, the dynamic simulation and calculation results of the short-circuit current of each phase of the IIDG with the change of the access capacity are calculated, as shown in Figure 10.

In the figure, when the two-phase-to-ground short-circuit fault occurs, the voltage drop of the IIDG terminal is more serious. At this time, the positive and negative sequence components of the short-circuit current are larger than those of the single-phase short-circuit.

Based on the above analysis, we can conclude that, after the improvement of the RLS algorithm, the calculation capability of the algorithm for short-circuit current of photovoltaic power plants has been improved. The calculation accuracy is improved by 14%, which effectively improves the problem of insufficient calculation accuracy of the previous RLS algorithm.

5. Conclusion

This paper is mainly to improve the short-circuit current calculation problem of photovoltaic power plants. For this reason, the RLS algorithm is introduced, and the calculation process and related steps of the algorithm are understood in detail. The current short-circuit problem of photovoltaic power plants is also understood, and the RLS algorithm is improved. The improved RLS algorithm can be better applied to the research topic of this paper in the practical model of short-circuit current calculation. Finally, related experiments are designed to calculate the short-circuit current, statistics of the current value, and memory analysis. Finally, it is concluded that the improved RLS algorithm can well improve the problem of insufficient calculation accuracy of the previous RLS algorithm in the actual short-circuit current calculation process and improve the calculation accuracy and calculation efficiency.

Data Availability

The data of this paper can be obtained upon request to the corresponding author via email.

Conflicts of Interest

The authors declare that there are no conflicts of interest regarding the publication of this work.

Acknowledgments

This work was supported by science and technology project of China Southern Power Grid Corporation (GXKJXM20200340).

References

[1] A. P. Vikharev, "Calculation of the admissible short circuit current for the protected wires of an ohl," *Power Technology and Engineering*, vol. 52, no. 3, pp. 357–360, 2018.

[2] J. Ma, Q. Liu, and J. Wu, "Three-phase short-circuit current calculation for power transmission system with high penetration of converter-type sources," *Dianli Xitong Zidonghua/ Automation of Electric Power Systems*, vol. 43, no. 5, 2019.

[3] W. Xie, M. Liu, and X. Zhou, "Short-circuit current calculation of inverter interfaced distributed generator based on voltage control in distribution network," *Journal of Chongqing University*, vol. 40, no. 2, pp. 70–79, 2017.

[4] C. Zhang, J. Zhang, and W. Zhao, "Fault characteristics of full power inverted sources and its short-circuit current calculation model," *Journal of Engineering*, vol. 2017, no. 13, 2476 pages, 2017.

[5] D. Sun, L. Liu, and Y. Zhang, "Recursive regularisation parameter selection for sparse RLS algorithm," *Electronics Letters*, vol. 54, no. 5, pp. 286-287, 2018.

[6] K. E. Vignesh, S. Akkara, and T. Jarin, "A revised RLS algorithm for low frequency electro mechanical oscillation," *Journal of Advanced Research in Dynamical and Control Systems*, vol. 11, no. 4, pp. 112–122, 2019.

[7] B. Kheireddine, B. Zoubida, and H. Tarik, "Improved version of teaching learning-based optimization algorithm using random local search," *COMPEL: The International Journal for Computation and Mathematics in Electrical & Electronic Engineering*, vol. 38, no. 3, pp. 1048–1060, 2019.

[8] P. Chuku, T. Olwal, and K. Djouani, "Adaptive array beamforming using an enhanced RLS algorithm," *International Journal on AdHoc Networking Systems*, vol. 8, no. 1, pp. 01–13, 2018.

[9] A. A. Alwan and A. Z. Abualkishik, "A proposed AI-based algorithm for safety detection and reinforcement of photovoltaic steel," *Journal of Intelligent Systems and Internet of Things*, vol. 4, no. 1, pp. 41–55, 2021.

[10] S. E. I. Chelli, A. Nemmour, M. Ahmed, A. Boussaid, and A Khezzar, "An effective approach for real-time parameters estimation of doubly-fed induction machine using forgetting factor RLS algorithm," *European Journal of Engineering Education*, vol. 22, no. 2, pp. 169–177, 2020.

[11] N. Li, L. Chen, and D. Xiang, "A study of numerical integration based on Legendre polynomial and RLS algorithm," *Numerical Algebra*, vol. 7, no. 4, pp. 457–464, 2017.

[12] Y. Pyo, K. Lee, and K. You, "Epicenter localization using RDOA based RLS algorithm," *Universal Journal of Mechanical Engineering*, vol. 5, no. 1, pp. 20–23, 2017.

[13] P. Thapa, H. I. Chang, and G. C. Park, "Performance comparison of RLS and LMS algorithm based cognitive radio for maximum energy detection in smart grid network," *International Journal of Tomography and Simulation*, vol. 30, no. 4, pp. 54–63, 2017.

[14] S. Y. Ma, B. Wang, and H. Peng, "l0-norm constraint RLS constant modulus algorithm for sparse channel equalization," *Tien Tzu Hsueh Pao/Acta Electronica Sinica*, vol. 45, no. 10, pp. 2561–2568, 2017.

[15] Y. Qiu, X. Li, and W. Chen, "Vanadium redox battery SOC estimation based on RLS and EKF algorithm," *Kongzhi yu Juece/Control and Decision*, vol. 33, no. 1, pp. 37–44, 2018.

[16] P. Wang, S. Wang, X. Zhang et al., "Rational construction of CoO/CoF2 coating on burnt-pot inspired 2D CNs as the battery-like electrode for supercapacitors," *Journal of Alloys and Compounds*, vol. 819, 2020.

[17] Z. Li, H. Yan, Y. Song, and J Guo, "Study on short circuit current calculation of power system with UHVDC and new energy source," *Energy and Power Engineering*, vol. 9, no. 4, pp. 625–634, 2017.

[18] C. Li and C. Zhao, "A Pole-to-Pole short-circuit fault current calculation method for DC grids," *IEEE Transactions on Power Systems*, vol. 32, no. 6, pp. 4943–4953, 2017.

[19] K. Chung, R. Y. Kim, H. Lee, and B. Kim, "Review of calculation method for short circuit current of AC railway feeders," *Journal of the Korean society for railway*, vol. 21, no. 9, pp. 859–869, 2018.

[20] B. Han, J. Li, J. Su, M. Guo, and B. Zhao, "Secrecy capacity optimization via cooperative relaying and jamming for WANETs," *IEEE Transactions on Parallel and Distributed Systems*, vol. 26, no. 4, pp. 1117–1128, 2015.

[21] C. Li, H. J. Yang, F. Sun, J. M. Cioffi, and L. Yang, "Multiuser overhearing for cooperative two-way multiantenna relays,"

IEEE Transactions on Vehicular Technology, vol. 65, no. 5, pp. 3796–3802, 2016.

[22] C. Li, F. Sun, J. M. Cioffi, and L. Yang, "Energy efficient MIMO relay transmissions via joint power allocations," *IEEE Transactions on Circuits and Systems II: Express Briefs*, vol. 61, no. 7, pp. 531–535, 2014.

[23] Z. Wang, J. Li, and T. Zheng, "Calculation and analysis of transient short circuit current of doubly-fed induction generator considering convertor current limitation and GSC current," *Diangong Jishu Xuebao/Transactions of China Electrotechnical Society*, vol. 33, no. 17, pp. 4123–4135, 2018.

[24] X. Kong, X. Zhang, X. Zhang, C. Wang, H. D. Chiang, and P Li, "Adaptive dynamic state estimation of distribution network based on interacting multiple model," *IEEE Transactions on Sustainable Energy*, vol. 13, no. 2, pp. 643–652, 2022.

[25] K. Guo, "Research on location selection model of distribution network with constrained line constraints based on genetic algorithm," *Neural Computing and Applications*, vol. 32, no. 6, pp. 1679–1689, 2020.

[26] H. Xu, S. Yang, and X. Jin, "A method to implement Ward equivalent based on power flow calculation and short circuit calculation," *Dianli Xitong Baohu yu Kongzhi/Power System Protection and Control*, vol. 46, no. 24, pp. 104–110, 2018.

[27] S. Gao and H. Ye, "Accurate and efficient estimation of short-circuit current for MTDC grids considering MMC control," *IEEE Transactions on Power Delivery*, vol. 35, no. 3, pp. 1541–1552, 2019.